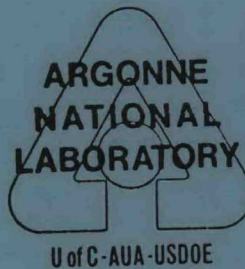


THERMODYNAMIC THEORY OF CAVITATION
NUCLEI IN DILUTE LIQUID-GAS SOLUTIONS

by

Y. S. Cha
Components Technology Division



MASTER

BASE TECHNOLOGY

June 1978

DISTRIBUTION OF THIS DOCUMENT IS UNLIMITED

DISCLAIMER

Portions of this document may be illegible in electronic image products. Images are produced from the best available original document.

The facilities of Argonne National Laboratory are owned by the United States Government. Under the terms of a contract (W-31-109-Eng-38) between the U. S. Department of Energy, Argonne Universities Association and The University of Chicago, the University employs the staff and operates the Laboratory in accordance with policies and programs formulated, approved and reviewed by the Association.

MEMBERS OF ARGONNE UNIVERSITIES ASSOCIATION

The University of Arizona	Kansas State University	The Ohio State University
Carnegie-Mellon University	The University of Kansas	Ohio University
Case Western Reserve University	Loyola University	The Pennsylvania State University
The University of Chicago	Marquette University	Purdue University
University of Cincinnati	Michigan State University	Saint Louis University
Illinois Institute of Technology	The University of Michigan	Southern Illinois University
University of Illinois	University of Minnesota	The University of Texas at Austin
Indiana University	University of Missouri	Washington University
Iowa State University	Northwestern University	Wayne State University
The University of Iowa	University of Notre Dame	The University of Wisconsin

NOTICE

This report was prepared as an account of work sponsored by the United States Government. Neither the United States nor the United States Department of Energy, nor any of their employees, nor any of their contractors, subcontractors, or their employees, makes any warranty, express or implied, or assumes any legal liability or responsibility for the accuracy, completeness or usefulness of any information, apparatus, product or process disclosed, or represents that its use would not infringe privately-owned rights. Mention of commercial products, their manufacturers, or their suppliers in this publication does not imply or connote approval or disapproval of the product by Argonne National Laboratory or the U. S. Department of Energy.

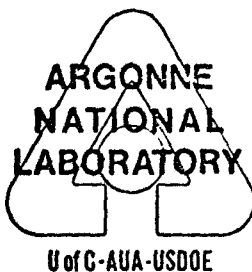
TECHNICAL MEMORANDUM

ANL-CT-78-33
ENGINEERING AND
EQUIPMENT (UC-38):
LMFBR COMPONENTS
(UC-79k)

THERMODYNAMIC THEORY OF CAVITATION
NUCLEI IN DILUTE LIQUID-GAS SOLUTIONS

by

Y. S. Cha
Components Technology Division



NOTICE

This report was prepared as an account of work sponsored by the United States Government. Neither the United States nor the United States Department of Energy, nor any of their employees, nor any of their contractors, subcontractors, or their employees, makes any warranty, express or implied, or assumes any legal liability or responsibility for the accuracy, completeness or usefulness of any information, apparatus, product or process disclosed, or represents that its use would not infringe privately owned rights.

BASE TECHNOLOGY

MASTER

June 1978

DISTRIBUTION OF THIS DOCUMENT IS UNLIMITED *eb*

TABLE OF CONTENTS

	<u>Page</u>
NOMENCLATURE	<i>i</i>
LIST OF FIGURES	<i>iii</i>
ABSTRACT	<i>iv</i>
I. INTRODUCTION	1
II. CONDITIONS OF EQUILIBRIUM	2
III. STABILITY CRITERIA	6
IV. NUMERICAL RESULTS	10
V. CAVITATION AND DISSOLUTION LIMITS	13
REFERENCES	16
APPENDIX A	17
APPENDIX B	19
APPENDIX C	21

NOMENCLATURE

A	Interfacial area, m^2
F	Helmholtz free energy, J
K_2	Henry's law constant between solute 2 and solvent 1, Pa
n	Number of moles, g-mol
N	Total number of moles (see equations 8 and 9), g-mol
p	Partial pressure of gases, Pa
p_v	Vapor pressure of the solvent under its own pressure with a flat interface, Pa
P	Pressure, Pa
r	Radius of the bubble, m
R	Universal gas constant, 8.313 J/g-mol/K
T	Absolute temperature, K
v	Molar specific volume, $m^3/g\text{-mol}$
V	Volume, m^3
x	Mole fraction, dimensionless
μ	Chemical potential, J/g-mol
μ_0	Chemical potential of the pure component, J/g-mol
σ	Surface tension, N/m
Subscripts	
1	Solvent component
2	Solute component
c	Condition of which a bubble starts to grow indefinitely
d	Condition at which a bubble starts to dissolve completely
i	Initial condition

NOMENCLATURE (Contd.)

Superscripts

- ' Liquid phase
- " Gas or vapor phase

LIST OF FIGURES

<u>Fig. No.</u>	<u>Title</u>	<u>Page</u>
1.	Variation of system pressure with equilibrium bubble radius for a $N_2 - H_2O$ system with $T = 293K$ and $N_1 = 10^{-10}$ g-mol for various values of N_2/N_1 .	22
2.	Variation of system pressure with equilibrium bubble radius for a $N_2 - H_2O$ system with $T = 293K$, $N_1 = 10^{-10}$ g-mol, and $N_2/N_1 = 10^{-4}$.	23
3.	Stability boundary calculated by employing equation (36) for a $N_2 - H_2O$ system at $T = 293K$ for various values of N_1 .	24
4.	Comparison between the stability boundary calculated by using equation (36) and the loci of maxima and minima calculated by using equation (37) for a $N_2 - H_2O$ system with $T = 293K$ and $N_1 = 10^{-10}$ g-mol.	25
5.	Variation of n_2'/n_1' with r for a $N_2 - H_2O$ system with $T = 293K$ and $N_1 = 10^{-10}$ g-mol.	26
6.	Variation of cavitation limit with initial radius of a bubble for a $N_2 - H_2O$ system with $T = 293K$ and $P_1' = 1.013 \times 10^5$ Pa for various values of N_1 .	27
7.	Variation of dissolution limit with initial radius of a bubble for a $N_2 - H_2O$ system with $T = 293K$ and $P_1' = 1.013 \times 10^5$ Pa for various values of N_1 .	28
8.	Comparison between the stability boundary calculated by using equation (36) and the loci of maxima and minima calculated by using equation (37) for a $CO_2 - Freon\ 21$ system with $T = 298K$ and $N_1 = 10^{-14}$ g-mol.	29
9.	Variation of n_2'/n_1' with r for a $CO_2 - Freon\ 21$ system with $T = 298K$ and $N_1 = 10^{-14}$ g-mol.	30
10.	Comparison between the stability boundary calculated by using equation (36) and the loci of maxima and minima calculated by using equation (37) for a $N_2 - H_2O$ system with $T = 293K$ and $N_1 = 10^{-14}$ g-mol.	31
11.	Variation of n_2'/n_1' with r for a $N_2 - H_2O$ system with $T = 293K$ and $N_1 = 10^{-14}$ g-mol.	32

ABSTRACT

The stability of a spherical bubble in a two-component two-phase system is examined by employing the thermodynamic theory of dilute solutions. It is shown that a bubble can remain in a state of stable equilibrium provided that the ratio of the total number of moles of the solute to the total number of moles of the solvent in the system is not extremely small and that the system pressure falls between an upper bound (dissolution limit) and a lower bound (cavitation limit). The results of the analysis provide a theoretical basis for the persistence of microbubbles in a saturated liquid-gas solution. Thus to a certain extent, the results also help to resolve the dilemma that exists in the field of cavitation due to (1) the necessity of postulating the existence of microbubbles; and (2) the lack of theoretical justification for the persistence of such bubbles in a liquid.

I. INTRODUCTION

It is well known that the theoretical tensile strength of a liquid is much larger than that usually observed. This discrepancy between theory and experimental observations of tensile strength can be resolved by postulating the existence of nuclei, or microbubbles, in the liquid.¹ However, gas bubbles are considered unstable since these bubbles grow indefinitely in a supersaturated solution and dissolve completely in an undersaturated solution. Even in a saturated solution, gas bubbles will dissolve because of surface tension according to the theoretical work reported by Epstein and Plesset.² However, their conclusion concerning the effect of surface tension on the stability of gas bubbles in a saturated solution is questionable since the approximate solution obtained by them does not satisfy the governing equation [Equation (31) of Reference 2] which indicates that the bubble is in a state of equilibrium when the initial concentration equals the saturation concentration of the solution. Although gas bubbles can remain in equilibrium in a saturated solution, the stability or instability of such bubbles in equilibrium states has never been established from a thermodynamic viewpoint. Numerous models were proposed in the past to explain the persistence of long-lived nuclei in a liquid.³ So far, the most plausible explanation is the one proposed by Harvey et al.;⁴ they suggested that nuclei could be stabilized in cracks on the surfaces of solid particles in the liquid. Solid particles tend to settle down and fall to the bottom of the liquid. However, if the solid particles were small enough, say less than 5×10^{-7} meters in radius, they can be maintained in suspension by the mechanism of Brownian motion.³ One of the important characteristics of cavitation is that the tensile strength or cavitation threshold tend to

increase as the waiting time increases. This effect is usually attributed to the presence of relatively large solid particles which tend to settle out in the liquid. However, as pointed out by Plesset¹, this behavior could be explained by the presence of undissolved bubbles rising out of the liquid or completely dissolving into solution. In addition, the "free nucleus" model is extremely useful in clarifying many of the complex phenomena associated with cavitation although there still remains considerable mystery about the nature of these microbubbles.³

In this paper, the mystery of these microbubbles will be unraveled partially by examining the stability of a spherical bubble in a saturated dilute liquid-gas solution. Conditions of equilibrium and stability criteria are derived for a two-component two-phase system by employing the thermodynamic theory of dilute solutions. Numerical examples are presented. The results show that, for a given two-component two-phase system, a "free" bubble can remain in a state of stable equilibrium in a saturated liquid-gas solution under certain circumstances which depend primarily on the system pressure, the radius of the bubble, and the total number of moles of the solute and the solvent in the system.

II. CONDITIONS OF EQUILIBRIUM

Consider a spherical bubble in a dilute liquid-gas solution. A solution is dilute when the amount of solute is small compared to the amount of solvent. Let the solution be composed of n_1' moles of solvent and n_2' moles of solute, then for dilute solutions,

$$n_2' \ll n_1', \quad (1)$$

where the superscript ' refers to the liquid phase of the system; and sub-

scripts 1 and 2 refer to the solvent and the solute, respectively. When the solution is sufficiently dilute and can be assumed to be ideal, the chemical potential of each component in the solution can be written as

$$\mu_1' = \mu_{01}' (T, P') + RT \ln x_1', \quad (2)$$

and

$$\mu_2' = \mu_{02}' (T, P') + RT \ln x_2', \quad (3)$$

where μ_1' and μ_2' are the chemical potentials of the solvent and the solute, respectively; μ_{01}' and μ_{02}' are the chemical potentials of the pure components 1 and 2, respectively; P' is the pressure in the liquid phase; R is the universal gas constant; T is the absolute temperature; and x_1' and x_2' are the mole fractions of the solvent and the solute, respectively.

Assuming that the spherical bubble contains a mixture of ideal gases, then the chemical potential of each component in the ideal mixture can be written as

$$\mu_1'' = \mu_{01}'' (T) + RT \ln p_1'', \quad (4)$$

and
$$\mu_2'' = \mu_{02}'' (T) + RT \ln p_2'', \quad (5)$$

where the superscript " refers to the gaseous phase of the system; μ_1'' and μ_2'' are the chemical potentials of components 1 and 2 in the gaseous phase, respectively; μ_{01}'' and μ_{02}'' are the chemical potentials of components 1 and 2 in its pure states at unit pressure (sometimes referred to as standard chemical potential), respectively; and p_1'' and p_2'' are the partial pressures of the components 1 and 2 in the ideal mixture, respectively.

During a reversible isothermal transformation, the variation in free energy of the system is

$$\begin{aligned}
dF &= dF' + dF'' + \sigma dA \\
&= -P' dV' + \mu_1' dn_1' + \mu_2' dn_2' - P'' dV'' \\
&\quad + \mu_1'' dn_1'' + \mu_2'' dn_2'' + \sigma dA,
\end{aligned} \tag{6}$$

where F is the Helmholtz free energy of the system; F' and F'' are the Helmholtz free energies of the liquid and the gaseous phases, respectively; σ is the surface tension; A is the interfacial area; P'' is the total pressure of the ideal gas mixture; V' and V'' are the volumes of the liquid and the gaseous phases, respectively; and n_1' and n_2'' are the number of moles of components 1 and 2 in the ideal mixture, respectively. The total volume of the system and the total number of moles of each component in the system remain constant during the transformation,

$$V' + V'' = \text{constant}, \tag{7}$$

$$n_1' + n_1'' = N_1 = \text{constant}, \tag{8}$$

and

$$n_2' + n_2'' = N_2 = \text{constant}. \tag{9}$$

In addition, we have

$$V'' = 4\pi r^3/3, \tag{10}$$

$$A = 4\pi r^2, \tag{11}$$

and

$$x_1' + x_2' = 1. \tag{12}$$

Substituting equations (7) through (11) into equation (6),

$$dF = (P' - P'' + 2\sigma/r) dV'' + (\mu_1'' - \mu_1') dn_1'' + (\mu_2'' - \mu_2') dn_2''. \tag{13}$$

The following equilibrium equations are obtained by letting $dF = 0$,

$$P' - P'' + 2\sigma/r = 0. \quad (14)$$

$$\mu_1' = \mu_1'', \quad (15)$$

and

$$\mu_2' = \mu_2''. \quad (16)$$

By assuming that the liquid is incompressible, it can be shown that equation (15) leads to the following equation (see APPENDIX A):

$$P_1'' = x_1' P_V \exp \left[v_1' (P' - P_V) / RT \right], \quad (17)$$

where P_V is the vapor pressure of the pure solvent over a flat interface; and v_1' is the molar specific volume of the solvent. For dilute solutions, x_1' is very close to unity. If the molar specific volume of the vapor of the solvent is large compared to that of the solvent, the difference between P_1'' and P_V will be small and can be neglected.

Substituting equations (3) and (5) into equation (16) we get:

$$P_2'' / x_2' = \exp \left[(\mu_{02}' - \mu_{02}'') / RT \right]. \quad (18)$$

In general, μ_{02}' is a function of temperature and pressure. However, if the solution is assumed to be incompressible, μ_{02}' becomes a function of temperature only,⁵ and equation (18) becomes,

$$P_2'' / x_2' = K_2(T), \quad (19)$$

where K_2 is the Henry's law constant between the solute and the solvent with a curved interface. It will be assumed that the effect of curvature on the solubility of the gas in the liquid is small and can be neglected. Thus, K_2 is taken to be the same as the Henry's law constant between the solute and the solvent with a flat interface (see APPENDIX B).

For dilute solutions, the following approximation can be employed for equation (19),

$$p_2'' = K_2 x_2^1 = K_2 n_2^1 / (n_1^1 + n_2^1) \approx K_2 n_2^1 / n_1^1 . \quad (20)$$

For the ideal mixture in the bubble,

$$P'' = p_1'' + p_2'' , \quad (21)$$

where

$$p_1'' = n_1'' RT / V'' , \quad (22)$$

$$p_2'' = n_2'' RT / V'' . \quad (23)$$

Substituting equations (20) and (23) into equation (9) and employing equations (8) and (22), it can be shown that

$$p_2'' = N_2 \left/ \left[N_1 / K_2 + V'' (1 - p_1'' / K_2) / RT \right] \right. . \quad (24)$$

Substituting equations (21) and (24) into equation (14),

$$P' = p_1'' + N_2 \left/ \left[N_1 / K_2 + V'' (1 - p_1'' / K_2) / RT \right] \right. - 2\sigma / r . \quad (25)$$

Equation (25) is the equilibrium equation which, together with equations (12), (17), (19), and (24), determines the equilibrium conditions of the system. It should be noted that equation (25) is different from the equilibrium equation reported by Mori, Hijikata, and Nagatani.⁶ They employed n_1^1 and n_2^1 , which are variables, in the equilibrium equation whereas equation (25) employs N_1 and N_2 which are constants for a given system.

If the gas is insoluble ($K_2 \rightarrow \infty$), equation (25) reduces to

$$P' = p_1'' + RTN_2 / V'' - 2\sigma / r . \quad (26)$$

III. STABILITY CRITERIA

Applying Taylor expansion to F,

$$\Delta F = dF + d^2F/2! + d^3F/3! + \dots,$$

where dF is given by equation (13) and determines the equilibrium conditions.

In order that the bubble be in a state of stable equilibrium, d^2F must be greater than zero. For the present system, it can be shown that

$$\begin{aligned} d^2F = & a_{11} (dV'')^2 + a_{12} dV''dn_1'' + a_{13} dV''dn_2'' \\ & + a_{21} dV''dn_1'' + a_{22} (dn_1'')^2 + a_{23} dn_1''dn_2'' \\ & + a_{31} dn_2''dV'' + a_{32} dn_2''dn_1'' + a_{33} (dn_2'')^2, \end{aligned} \quad (27)$$

where

$$a_{11} = \left[\frac{\partial(2\sigma/r - P'')}{\partial V''} \right]_{n_1'', n_2''} - \left(\frac{\partial P'}{\partial V'} \right)_{n_1', n_2'}, \quad (28a)$$

$$a_{22} = \left(\frac{\partial \mu_1'}{\partial n_1'} \right)_{n_2', V'} + \left(\frac{\partial \mu_1''}{\partial n_1''} \right)_{n_2'', V''}, \quad (28b)$$

$$a_{33} = \left(\frac{\partial \mu_2'}{\partial n_2'} \right)_{V', n_1'} + \left(\frac{\partial \mu_2''}{\partial n_2''} \right)_{V'', n_1''}, \quad (28c)$$

$$a_{12} = a_{21} = \left(\frac{\partial \mu_1'}{\partial V'} \right)_{n_1', n_2'} + \left(\frac{\partial \mu_1''}{\partial V''} \right)_{n_1'', n_2''}, \quad (28d)$$

$$a_{23} = a_{32} = \left(\frac{\partial \mu_1'}{\partial n_2'} \right)_{V', n_1'} + \left(\frac{\partial \mu_1''}{\partial n_2''} \right)_{V'', n_1''}, \quad (28e)$$

$$a_{13} = a_{31} = \left(\frac{\partial \mu_2'}{\partial V'} \right)_{n_1', n_2'} + \left(\frac{\partial \mu_2''}{\partial V''} \right)_{n_1'', n_2''}. \quad (28f)$$

Equation (27) is of the quadratic form in variables dV'' , dn_1'' , and dn_2'' . This quadratic form must be positive-definite in order to make $d^2F > 0$. A necessary

and sufficient condition that the quadratic form be positive-definite is given by the following expressions:

$$a_{11} > 0, \quad (29)$$

$$\begin{vmatrix} a_{11} & a_{12} \\ a_{21} & a_{22} \end{vmatrix} > 0, \quad (30)$$

and

$$\begin{vmatrix} a_{11} & a_{12} & a_{13} \\ a_{21} & a_{22} & a_{23} \\ a_{31} & a_{32} & a_{33} \end{vmatrix} > 0. \quad (31)$$

Employing equations (2) to (5) and the assumption that the liquid is incompressible, it can be shown that

$$\left(\frac{\partial P'}{\partial V'} \right)_{n_1^i, n_2^i} = 0, \quad (32a)$$

$$\left[\frac{\partial(2\sigma/r - P'')}{\partial V''} \right]_{n_1^{ii}, n_2^{ii}} = P''/V'' - 2\sigma/(3rV''), \quad (32b)$$

$$\left(\frac{\partial \mu_1^i}{\partial n_1^i} \right)_{n_2^i, V'} = RT x_2^i/n_1^i, \quad (32c)$$

$$\left(\frac{\partial \mu_1^{ii}}{\partial n_1^{ii}} \right)_{n_2^{ii}, V''} = RT/n_1^{ii}, \quad (32d)$$

$$\left(\frac{\partial \mu_2^i}{\partial n_2^i} \right)_{V', n_1^i} = RT x_1^i/n_2^i, \quad (32e)$$

$$\left(\frac{\partial \mu_2''}{\partial n_2''}\right)_{V'', n_1''} = RT/n_2'' , \quad (32f)$$

$$\left(\frac{\partial \mu_1'}{\partial V'}\right)_{n_1', n_2'} = \left(\frac{\partial \mu_2'}{\partial V'}\right)_{n_1', n_2'} = \left(\frac{\partial \mu_1''}{\partial n_2''}\right)_{V'', n_1''} = 0, \quad (32g)$$

$$\left(\frac{\partial \mu_1''}{\partial V''}\right)_{n_1'', n_2''} = \left(\frac{\partial \mu_2''}{\partial V''}\right)_{n_1'', n_2''} = -RT/V'' , \quad (32h)$$

$$\left(\frac{\partial \mu_1'}{\partial n_2'}\right)_{V', n_1'} = -RT/(n_1' + n_2'). \quad (32i)$$

Substituting equations (14), (28), and (32) into the inequalities (29), (30), and (31), the stability criteria becomes,

$$P' > -4\sigma/3r, \quad (29a)$$

$$P' > p_1'' \left/ \left[x_1' + x_2' N_1 / (N_1 - p_1'' V'' / RT) \right] - 4\sigma/3r, \quad (30a)\right.$$

and

$$P' > (x_2' p_2'' N_1 + x_1' p_1'' N_2) / (x_1'^2 N_2 + x_2'^2 N_1) - 4\sigma/3r. \quad (31a)$$

Since the first terms on the righthand sides of (30a) and (31a) are positive quantities, it is obvious that (30a) and (31a) are more stringent than (29a).

To compare (30a) with (31a), let

$$P'_a = p_1'' \left/ \left[x_1' + x_2' N_1 / (N_1 - p_1'' V'' / RT) \right] - 4\sigma/3r ,\right.$$

and

$$P'_b = (x_2' p_2'' N_1 + x_1' p_1'' N_2) / (x_1'^2 N_2 + x_2'^2 N_1) - 4\sigma/3r. \quad (33)$$

It can be shown that,

$$P'_b - P'_a = \frac{x_2' n_1' N_1 p_2'' (1 - x_2' - p_1'' / K_2) + x_2'^2 N_1^2 p_2'' + x_1' x_2' N_1 N_2 p_1''}{(x_1'^2 N_2 + x_2'^2 N_1) (n_1' x_1' + N_1 x_2')} .$$

Thus, $P'_b > P'_a$ provided that the following condition is satisfied,

$$1 - x_2^1 - p_1''/K_2 > 0. \quad (34)$$

K_2 is usually very large compared to p_1'' and x_2^1 is small compared to unity for dilute solutions. Therefore, (34) is satisfied for most practical applications. Under such circumstances, (31a) alone is sufficient to determine the stability of the system.

If the gas is insoluble ($x_1^1 = 1$ and $x_2^1 = 0$), P'_a becomes equal to P'_b ,

$$P'_a = P'_b = p_1'' - 4\sigma/3r. \quad (35)$$

Equation (35), together with equation (26), gives the critical pressure below which there is no equilibrium radius for a bubble. This result, which is a special case of the present analysis, has been frequently employed to explain the onset of cavitation in a liquid.^{3,7}

IV. NUMERICAL RESULTS

As an example, the results of a nitrogen (solute) and water (solvent) system will be presented. Numerical constants employed in the calculations are: $T = 293\text{K}$, $p_v = 2.337 \times 10^3 \text{ Pa}$, $R = 8.313 \text{ J/g-mol/K}$, $\sigma = 7.32 \times 10^{-2} \text{ N/m}$, and $K_2 = 8.13 \times 10^8 \text{ Pa}$. At this temperature, p_1'' is nearly equal to p_v . Therefore, only equation (25) is needed to calculate the equilibrium radii for given values of P' , N_1 , and N_2 . It is also obvious that K_2 is much larger than p_1'' and (34) is satisfied. The stability of the system is then determined by (31a).

Figure 1 shows the typical variation of system pressure (P') with equilibrium radius for given values of N_1 and N_2 calculated by employing equation (25). The dashed line in Fig. 1 is the limiting conditions obtained by letting

$$P' = P'_b, \quad (36)$$

where P' and P'_b are given by equations (25) and (33), respectively. Stability criterion (31a) indicates that the equilibria are stable if the slopes of the equilibrium curves in Fig. 1 are negative ($\partial P'/\partial r < 0$) and the equilibria are unstable if the slopes of the equilibrium curves are positive ($\partial P'/\partial r > 0$).

For example, Fig. 2 shows the stable and unstable regions of a particular case ($N_2/N_1 = 10^{-4}$) in Fig. 1. If the ratio of N_2/N_1 is relatively small, say less than 5×10^{-5} in Fig. 1, the equilibria are always unstable. As the ratio of N_2/N_1 is increased beyond 5×10^{-5} , the equilibria can either be stable or unstable, and the stability of the equilibrium depends on the values of r and P' . The dashed line in Fig. 1 provides the stability boundary for a given value of N_1 . The upper right corner bounded by the dashed line in Fig. 1 is in the stable equilibrium region and the rest of the area is in the unstable equilibrium region. By varying the value of N_1 , a number of stability boundaries can be generated and they are shown in Fig. 3. For relatively large values of N_1 ($> 10^{-5}$ g-mol), only relatively large bubbles can remain in stable equilibria when the system pressure is above the vapor pressure of the solvent and no bubble can remain in stable equilibrium when the system pressure is below the vapor pressure of the solvent. As N_1 is decreased, smaller bubbles can remain in stable equilibria even when the system pressure is negative.

It is obvious from Fig. 3 that, depending on the value of N_1 , bubbles with radii as small as 10^{-7} m and as large as 10^{-2} m can remain in stable equilibria in the absence of gravity. In practice, however, larger bubbles tend to rise to the surface and only very small bubbles with radii in the order of $r = 10^{-7}$ m can be maintained in suspension by the mechanism of Brownian motion as mentioned previously. Larger bubbles rise faster than smaller bubbles.

For example, it takes approximately thirty seconds for a bubble with a radius of 10^{-4} m to rise a distance of one meter, whereas it may take one hundred hours for a bubble with a radius of 10^{-6} m to rise the same distance. Thus, in a system that contains microbubbles of various sizes in stable thermodynamic equilibria, this "aging effect" is inevitable. In order to obtain consistent results in laboratory tests, sufficient waiting time must be allowed so that only extremely small bubbles with radii in the order of 10^{-7} m can remain in the liquid. In summary, the results of the present analysis provide a theoretical basis for the persistence of microbubbles in a saturated liquid-gas solution and a possible explanation of the "aging effect" in such a solution.

It can be observed from Fig. 1 that the stability boundary calculated by employing equation (36) appears to coincide with the loci of maxima and minima of the equilibrium curves. The loci of maxima and minima of the equilibrium curves in Fig. 1 can be obtained by setting $\partial P'/\partial r$ equal to zero in equation (25),

$$(\partial P'/\partial r)_{N_1, N_2} = 2\sigma/r^2 - 4\pi r^2 P_2^2 (1 - P_1/K_2)/(N_2 RT) = 0. \quad (37)$$

It is obvious that equations (36) and (37) are not identical. Figure 4 shows the comparison between the stability boundary obtained by employing equation (36) and the loci of maxima and minima of the equilibrium curves obtained by employing equation (37) for $N_1 = 10^{-10}$ g-mol over a wide range of system pressure. When the bubble is relatively large and the system pressure is relatively low, the difference between equation (36) and equation (37) is negligible. This difference increases as the bubble becomes smaller and the system pressure becomes higher. The basic assumption made in the present analysis is that the solution be dilute so that the inequality (1) can be satisfied. This assumption requires that the system pressure be relatively low so that the solution can

remain dilute. Figure 5 shows the variation of the ratio n_2'/n_1' with r for the same case as that shown in Fig. 4 with $N_1 = 10^{-10}$ g-mol. It is obvious that n_2'/n_1' increases as r decreases for a given value of N_1 . Figure 4 indicates that deviation between equations (36) and (37) begins to appear when r approaches 10^{-6} m. At this radius, it can be observed from Fig. 5 that the ratio n_2'/n_1' becomes very large and the assumption expressed by the inequality (1) can no longer be satisfied. However, as long as the solution is dilute and the inequality (1) is strictly satisfied, the difference between equation (36) and equation (37) is small and can be neglected. Under such circumstance, (31a) becomes equivalent to

$$(\partial P'/\partial r)_{N_1, N_2} < 0, \quad (38)$$

and the stability of the system can be determined directly by examining the equilibrium curves without employing (31a). This result was found to be valid for other values of N_1 in a nitrogen-water system and for other combinations of solute and solvent (see APPENDIX C).

V. CAVITATION AND DISSOLUTION LIMITS

Based on the equilibrium theory described previously, a cavitation and a dissolution limit can be defined. Referring to Fig. 2, if a bubble is initially in a state of stable equilibrium, then the relative minimum corresponds to the lowest pressure and the relative maximum corresponds to the highest pressure that such a bubble can remain in stable equilibrium. The minimum pressure can be considered as the highest pressure required to initiate the indefinite growth of the bubble and therefore will be defined as the cavitation limit (P'_c) of the bubble. The maximum pressure can be considered as the lowest pressure required to dissolve completely the bubble and therefore

will be defined as the dissolution limit (P'_d) of the bubble. It can be observed from Fig. 1 that P'_c and P'_d are functions of N_1 and N_2 . For a given value of N_1 , Fig. 1 indicates that a system with a smaller value of N_2 has lower values of P'_c and P'_d compared to systems with higher values of N_2 . Instead of calculating P'_c and P'_d in terms of N_1 and N_2 , an alternate approach will be adopted. If a bubble is initially in a state of equilibrium, from equation (25),

$$P'_i = p_1'' - 2\sigma/r_i + N_2 \left/ \left[N_1/K_2 + 4\pi r_i^3(1 - p_1''/K_2)/(3RT) \right] \right., \quad (39)$$

where P'_i is the initial system pressure; and r_i is the initial radius of the bubble. Let r_c and r_d be the two positive solutions of equation (36) with $r_c > r_d$, then

$$P'_c = p_1'' - 2\sigma/r_c + N_2 \left/ \left[N_1/K_2 + 4\pi r_c^3(1 - p_1''/K_2)/(3RT) \right] \right., \quad (40)$$

and

$$P'_d = p_1'' - 2\sigma/r_d + N_2 \left/ \left[N_1/K_2 + 4\pi r_d^3(1 - p_1''/K_2)/(3RT) \right] \right., \quad (41)$$

For given values of P'_i , r_i , and N_1 , equation (39) can be used to calculate N_2 , and equations (36), (40), and (41) can then be employed to calculate r_c , r_d , P'_c , and P'_d . Results of such calculations for a $N_2 - H_2O$ system initially at atmospheric pressure and room temperature are shown in Fig. 6 and Fig. 7. In Fig. 6, values of $-(P'_c - p_1'')$ are plotted against r_i on a log-log paper. The reason for using $-(P'_c - p_1'')$ instead of $-P'_c$ is to avoid passing through zero on a log scale. As shown in Fig. 6, there is a curve associated with each value of N_1 and each curve has a relative maximum. However, bubbles with initial radii less than the radius at the maximum point are unstable (dashed lines in Fig. 6) and therefore can not be expected to exist if sufficient time

were allowed to eliminate these bubbles. For bubbles that are initially in a state of stable equilibrium, it can be observed from Fig. 6 that, for a given value of N_1 , the smaller the initial radius of the bubble, the lower the cavitation limit. In other words, a system that contains smaller bubbles can withstand a higher tension. Also shown in Fig. 6 is the cavitation limit calculated by employing equations (35) and (26) for the special case of an insoluble gas. For a given value of N_1 , the difference in cavitation limit between a soluble and an insoluble gas is small when the initial radius of the bubble is relatively large. This difference increases as r_i is decreased.

Figure 7 shows the variations of the dissolution limits with the initial radius of the bubble. Again, the dashed line to the left of the minimum point of each curve is in the unstable equilibrium region and should not be expected to exist if sufficient time were allowed to eliminate these bubbles. The solid curves in Fig. 7 indicate that the pressure required to force a bubble into solution increases with r_i for a given value of N_1 . In other words, it requires a higher pressure to dissolve a larger bubble in a given system.

The foregoing examples provide the means of determining the cavitation and the dissolution limits of a bubble at a given system temperature. Similar calculations can be performed to determine the relation between the system temperature and the equilibrium bubble radius at a given system pressure provided that the variations of K_2 , σ , p_v , and v_l' with temperature are known. This would enable one to determine the amount of superheat and subcooling that a bubble can sustain at a given system pressure.

REFERENCES

1. M. S. Plesset, NASA SP-304, Part I, 341 (1970).
2. P. S. Epstein and M. S. Plesset, J. Chem. Phys. 18, 1505 (1950).
3. H. G. Flynn, Physical Acoustics IB (W. P. Mason, Ed., Academic Press, New York, 1965), p. 58.
4. E. N. Harvey, D. K. Barnes, W. D. Mc Elroy, A. H. Whiteley, D. C. Pease, and K. W. Cooper, J. Cell. Comp. Physiol. 24, 1 (1944).
5. E. Fermi, Thermodynamics, (Dover Publications, New York, N.Y., 1956), Chap. VII.
6. Y. Mori, K. Hijikata, and T. Nagatani, Int. J. Heat Mass Transfer 20, 41 (1977).
7. R. T. Knapp, J. W. Daily, and F. G. Hammitt, Cavitation, (McGraw-Hill, New York, 1970), Chap. 3.

APPENDIX A - DERIVATION OF THE RELATIONSHIP BETWEEN p_1'' AND p_v

In order to obtain equation (17), we start with equation (15)

$$\mu_1^I = \mu_1^{II} .$$

It follows that,

$$d\mu_1^I = d\mu_1^{II} . \quad (A1)$$

For an isothermal transformation,

$$d\mu_1^I = (\partial\mu_1^I/\partial P^I) dP^I + (\partial\mu_1^I/\partial x_1^I) dx_1^I = v_1^I dP^I + (RT/x_1^I) dx_1^I , \quad (A2)$$

and

$$d\mu_1^{II} = (\partial\mu_1^{II}/\partial p_1^{II}) dp_1^{II} = (RT/p_1^{II}) dp_1^{II} . \quad (A3)$$

Substituting equations (A2) and (A3) into equation (A1),

$$v_1^I dP^I + (RT/x_1^I) dx_1^I = (RT/p_1^{II}) dp_1^{II} . \quad (A4)$$

If the liquid is incompressible, equation (A4) can be integrated directly,

$$v_1^I (P^I - P_0^I) + RT \ln x_1^I = RT \ln(p_1^{II}/p_1^{II_0}) ,$$

or

$$p_1^{II} = x_1^I p_1^{II_0} \exp \left[v_1^I (P^I - P_0^I) / RT \right] , \quad (A5)$$

where $p_1^{II_0}$ is the vapor pressure of the pure solvent over a curved interface; and P_0^I is the corresponding pressure of the solvent in its pure state. $p_1^{II_0}$ can be expressed in terms of p_v by employing the Kelvin equation,

$$p_1^{II_0} = p_v \exp \left[v_1^I (P_0^I - p_v) / RT \right] . \quad (A6)$$

Substituting equation (A6) into equation (A5),

$$p_i'' = x_i' p_v \exp \left[v_i' (P' - p_v) / RT \right]. \quad (A7)$$

Equation (A7) is the same as equation (17).

APPENDIX B - EFFECT OF CURVATURE ON THE SOLUBILITY OF A GAS IN A LIQUID

It follows from equation (16) that between the equilibrium of the solute in the two phases,

$$d\mu_2^l = d\mu_2^g . \quad (B1)$$

For an isothermal transformation,

$$d\mu_2^l = (\partial\mu_2^l/\partial P') dP' + (\partial\mu_2^l/\partial x_2^l) dx_2^l = v_2^l dP' + (RT/x_2^l) dx_2^l , \quad (B2)$$

and

$$d\mu_2^g = (\partial\mu_2^g/\partial p_2^g) dp_2^g = v_2^g dp_2^g = (RT/p_2^g) dp_2^g , \quad (B3)$$

where v_2^l and v_2^g are the molar specific volumes of the solute in the liquid and gas phases, respectively. Substituting equations (B2) and (B3) into equation (B1),

$$v_2^l dP' + (RT/x_2^l) dx_2^l = (RT/p_2^g) dp_2^g . \quad (B4)$$

Assuming that v_2^l is independent of P' , equation (B4) can be integrated,

$$v_2^l (P' - P_\infty^l) + RT \ln(x_2^l/x_{2,\infty}^l) = RT \ln(p_2^g/p_{2,\infty}^g) ,$$

or

$$\ln \left[(p_2^g/x_2^l) / (p_{2,\infty}^g/x_{2,\infty}^l) \right] = v_2^l (P' - P_\infty^l) / RT , \quad (B5)$$

where the subscript ∞ refers to the condition of a flat interface. The difference between P' and P_∞^l is due to the presence of a curved interface, thus,

$$P' - P_\infty^l = -2\sigma/r . \quad (B6)$$

Introducing the following Henry's law constants,

$$p_2''/x_2^I = K_2,$$

and

$$p_{2,\infty}''/x_{2,\infty}^I = K_{2,\infty}. \quad (B7)$$

Substituting equations (B6) and (B7) into equation (B5),

$$K_2/K_{2,\infty} = \exp \left[-2\sigma v_2^I / (rRT) \right], \quad (B8)$$

where v_2^I is the molar specific volume of the solute in the dissolved state. Since dissolved molecules generally bear a greater resemblance to liquid molecules than to those in the gaseous state, v_2^I is expected to be a small quantity under most circumstances. Thus, if r is not extremely small, the difference between K_2 and $K_{2,\infty}$ can be neglected. This requirement is comparable with another requirement, i.e., that the radius of the bubble be large compared with the thickness of a few molecules (10^{-9} m) so that surface tension is independent of the radius of curvature of the interface, which is also necessary in the present analysis.

APPENDIX C - DIFFERENCE BETWEEN EQUATION (36) AND EQUATION (37) FOR A HIGHLY SOLUBLE GAS

The difference between equation (36) and equation (37) depends not only on N_1 and N_2 , but also on K_2 , σ , etc. As an additional example, we shall consider the case of a highly soluble gas, such as CO_2 in Freon 21. Numerical constants employed in the calculations are: $T = 298\text{K}$, $p_v = 1.827 \times 10^5 \text{ Pa}$, $\sigma = 1.80 \times 10^{-2} \text{ N/m}$, and $K_2 = 1.274 \times 10^7 \text{ Pa}$. Figure 8 shows the comparison between the results obtained by employing equations (36) and (37) for a CO_2 - Freon 21 system with $N_1 = 10^{-14} \text{ g-mol}$. The corresponding variation of n_2/n_1 with r is shown in Fig. 9. For the purpose of comparison, the results of a N_2 - H_2O system with $N_1 = 10^{-14} \text{ g-mol}$ are shown in Fig. 10 and Fig. 11. Figure 8 indicates that the difference between equation (36) and equation (37) for a CO_2 - Freon 21 system begins to appear at a system pressure equal to approximately 2.3 atmospheres. As can be observed from Fig. 10, the difference between equation (36) and equation (37) for a N_2 - H_2O system begins to appear at a system pressure of approximately 30 atmospheres. As mentioned in Section IV, when the difference between equation (36) and equation (37) begins to appear, the assumption of dilute solution expressed by the inequality (1) can no longer be satisfied strictly. This is also true for the cases shown in Figs. 8 and 9, and in Figs. 10 and 11. Therefore, for a highly soluble gas, the pressure limit below which the present analysis applies is much lower than the case of a less soluble gas.

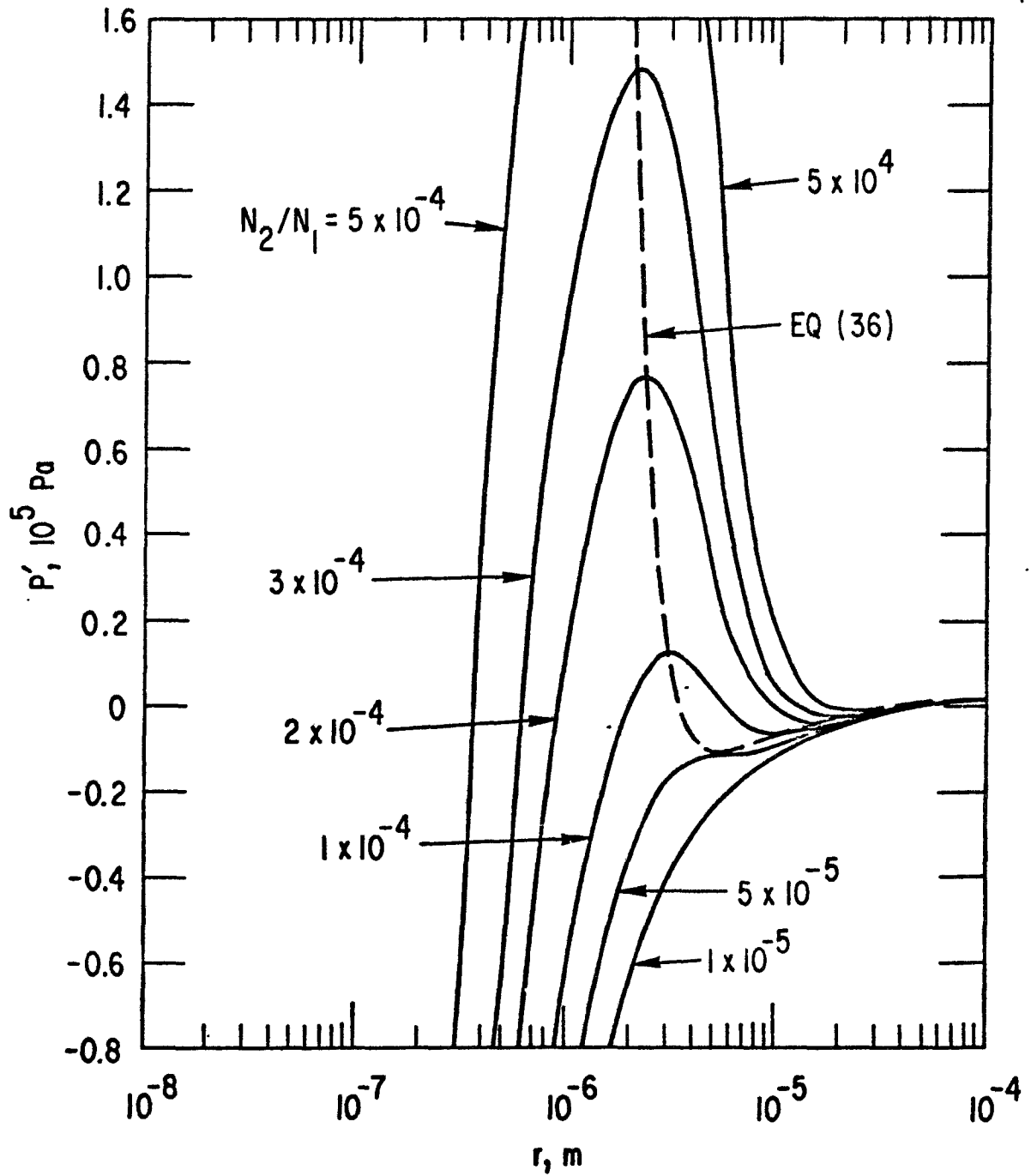


Fig. 1. Variation of system pressure with equilibrium bubble radius for a $N_2 - H_2O$ system with $T = 293K$ and $N_1 = 10^{-10}$ g-mol for various values of N_2/N_1 .

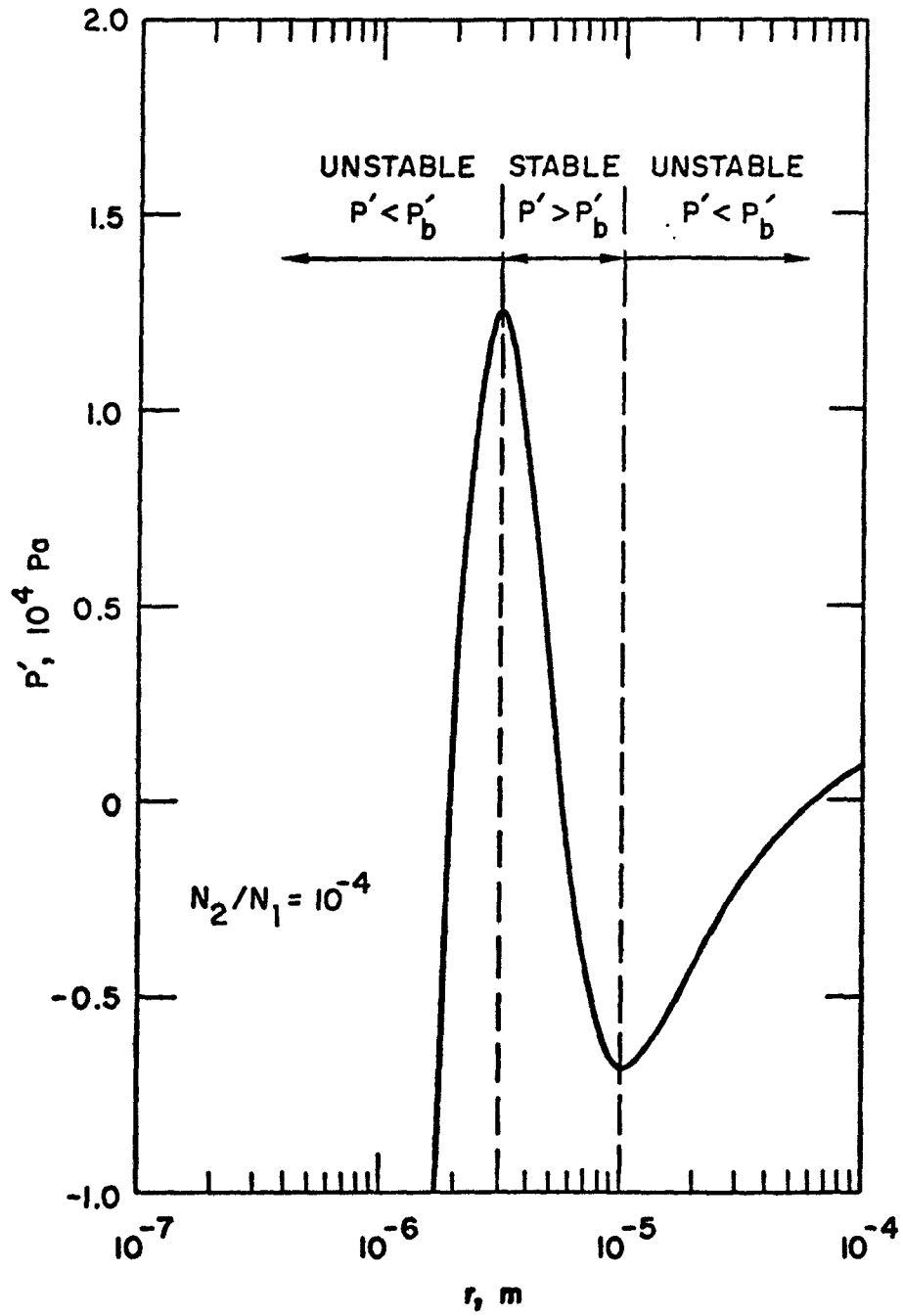


Fig. 2. Variation of system pressure with equilibrium bubble radius for a $N_2 - H_2O$ system with $T = 293K$, $N_1 = 10^{-10}$ g-mol, and $N_2/N_1 = 10^{-4}$.

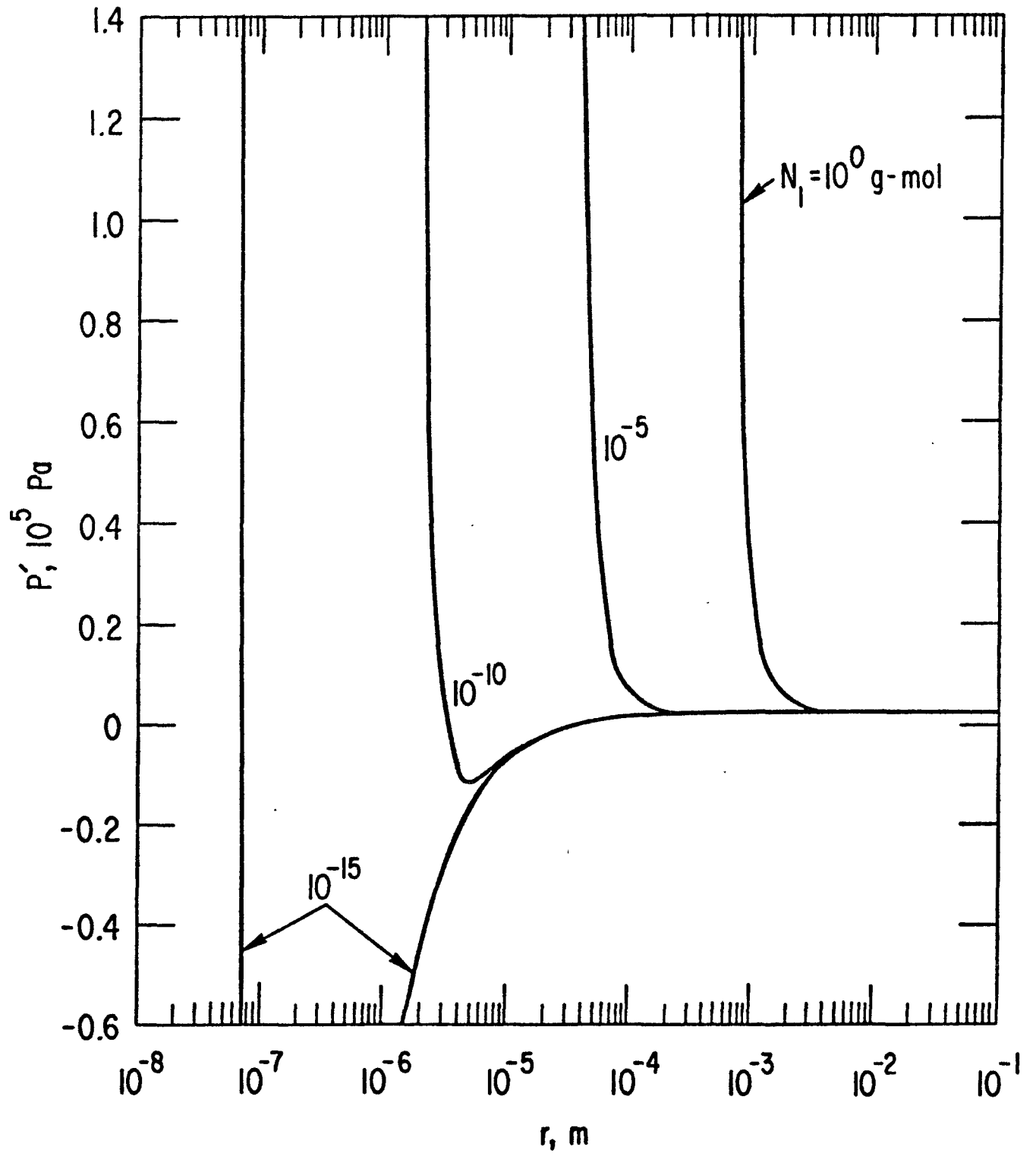


Fig. 3. Stability boundary calculated by employing equation (36) for a $N_2 - H_2O$ system at $T = 293K$ for various values of N_1 .

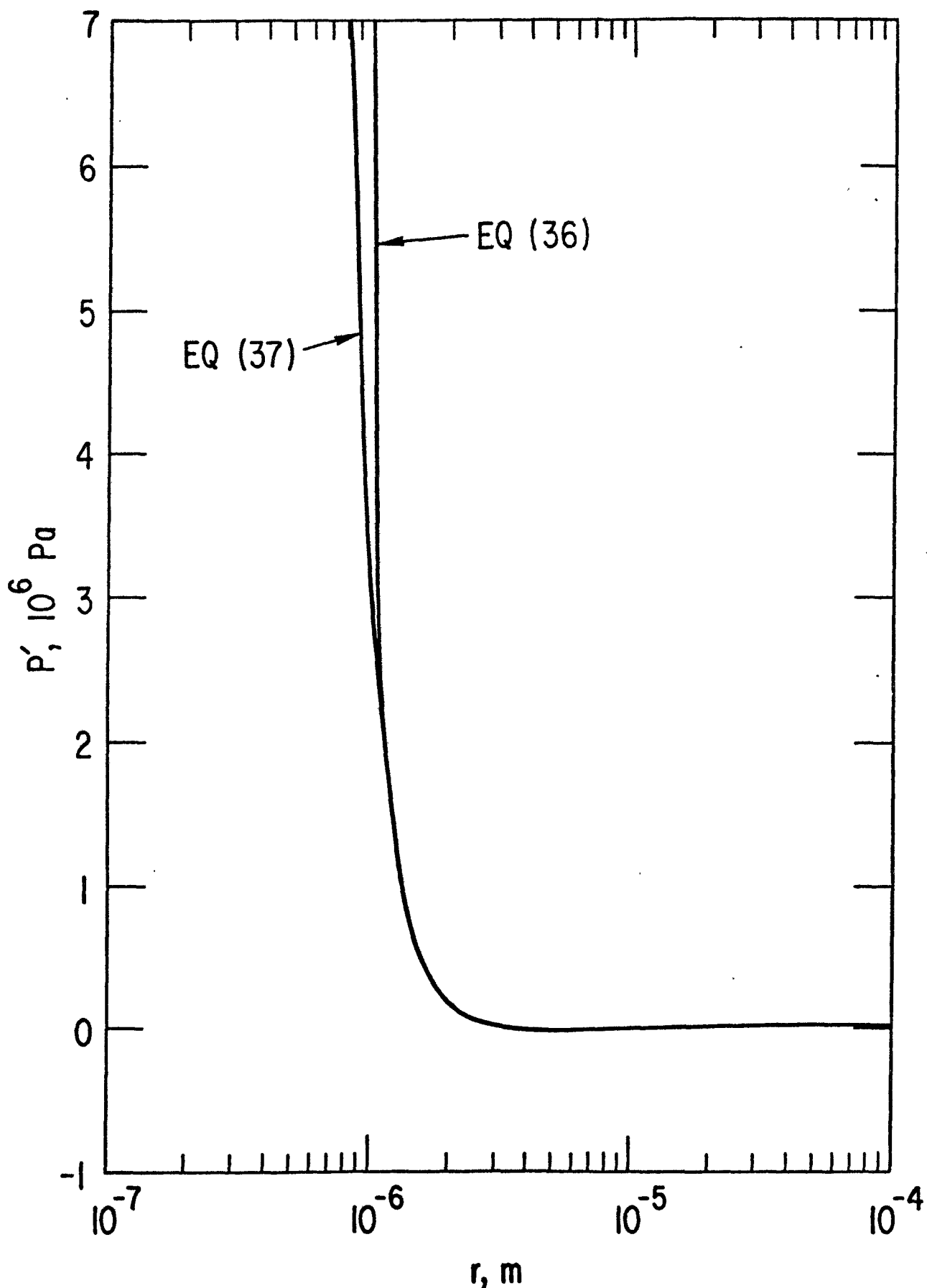


Fig. 4. Comparison between the stability boundary calculated by using equation (36) and the loci of maxima and minima calculated by using equation (37) for a $\text{N}_2 - \text{H}_2\text{O}$ system with $T = 293\text{K}$ and $N_1 = 10^{-10} \text{ g-mol}$.

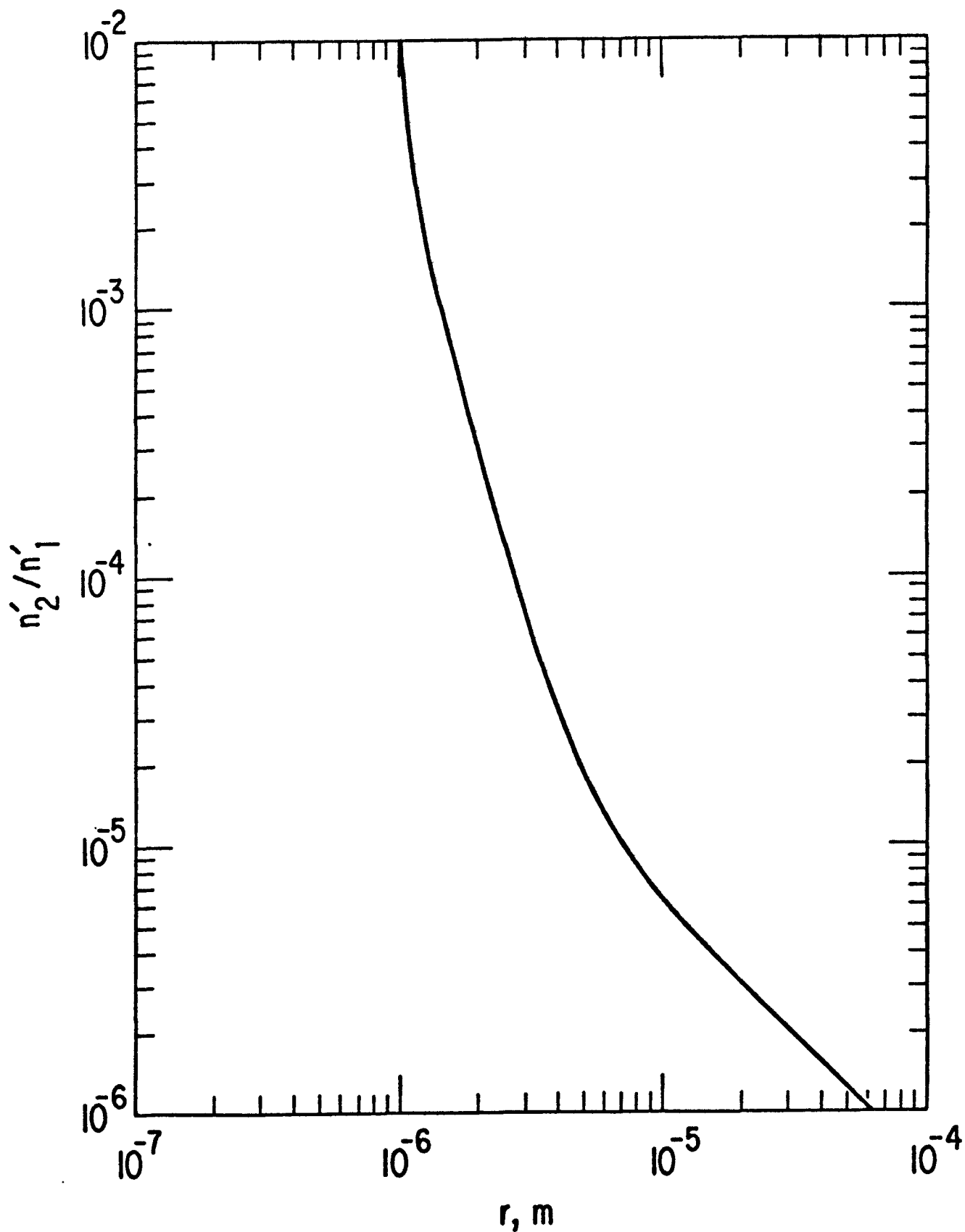


Fig. 5. Variation of n'_2/n'_1 with r for a $N_2 - H_2O$ system with $T = 293K$ and $N_1 = 10^{-10}$ g-mol.

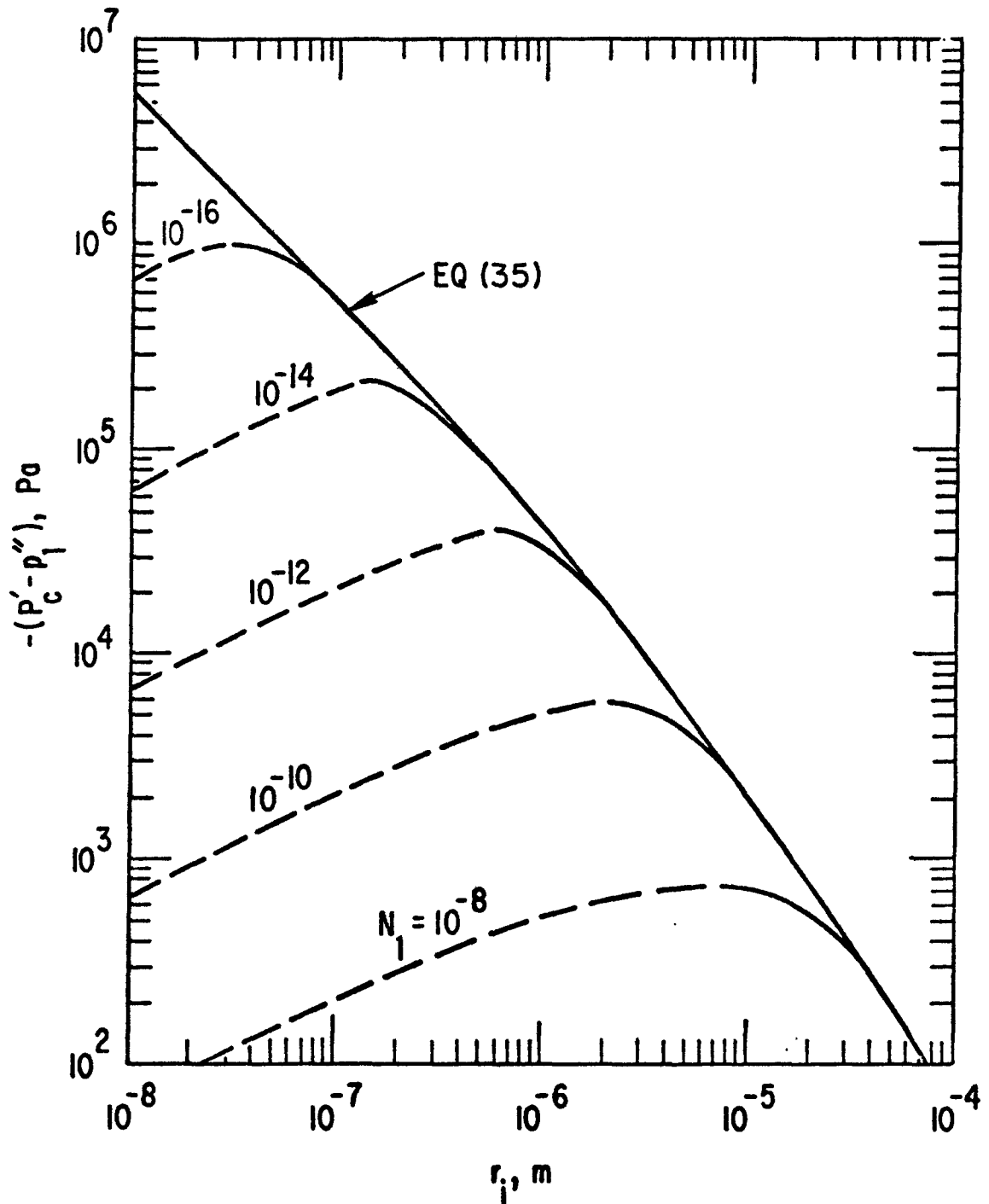


Fig. 6. Variation of cavitation limit with initial radius of a bubble for a $\text{N}_2 - \text{H}_2\text{O}$ system with $T = 293\text{K}$ and $P'_i = 1.013 \times 10^5 \text{ Pa}$ for various values of N_1 .

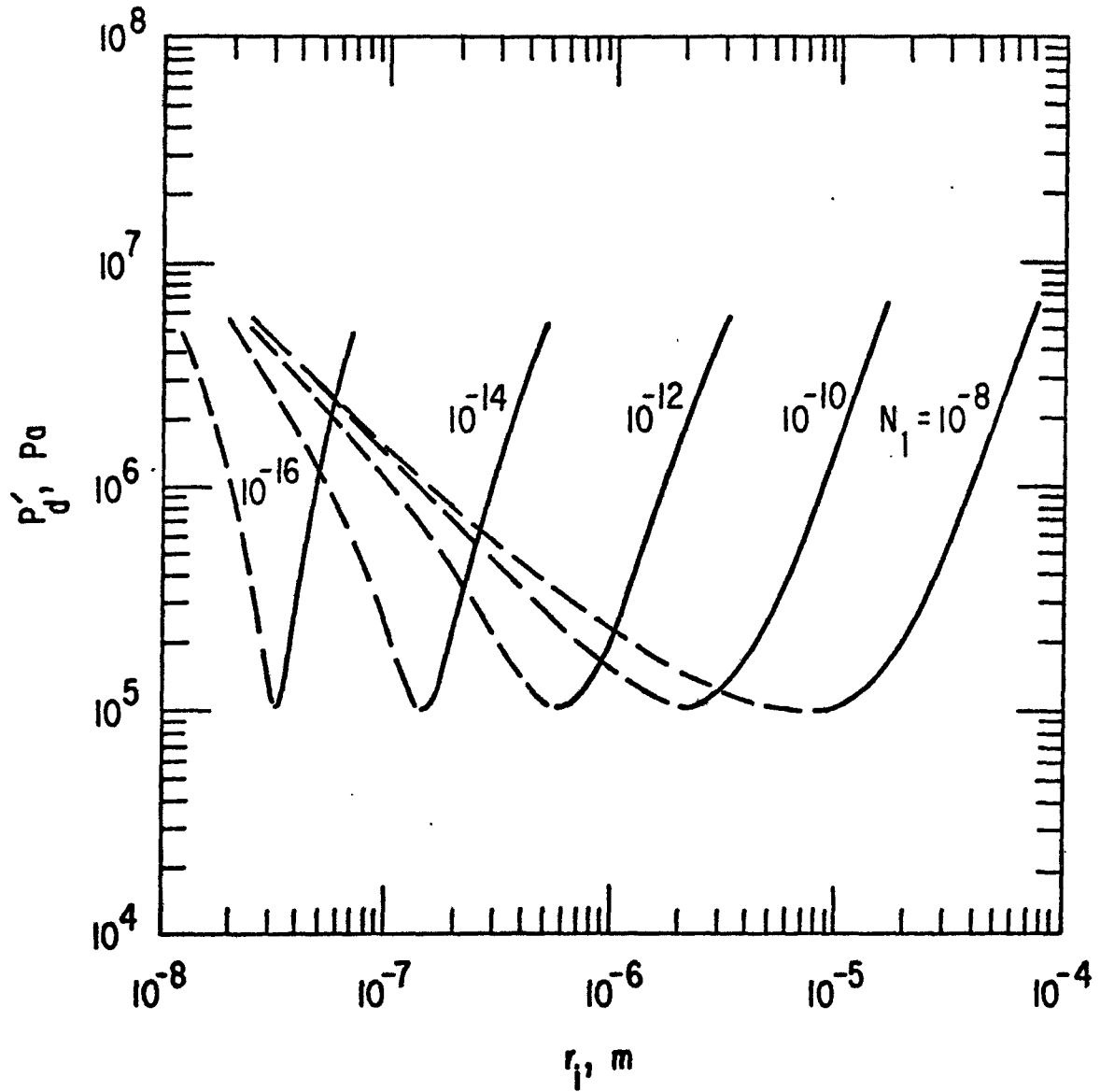


Fig. 7. Variation of dissolution limit with initial radius of a bubble for a $\text{N}_2 - \text{H}_2\text{O}$ system with $T = 293\text{K}$ and $P_i' = 1.013 \times 10^5 \text{ Pa}$ for various values of N_1 .

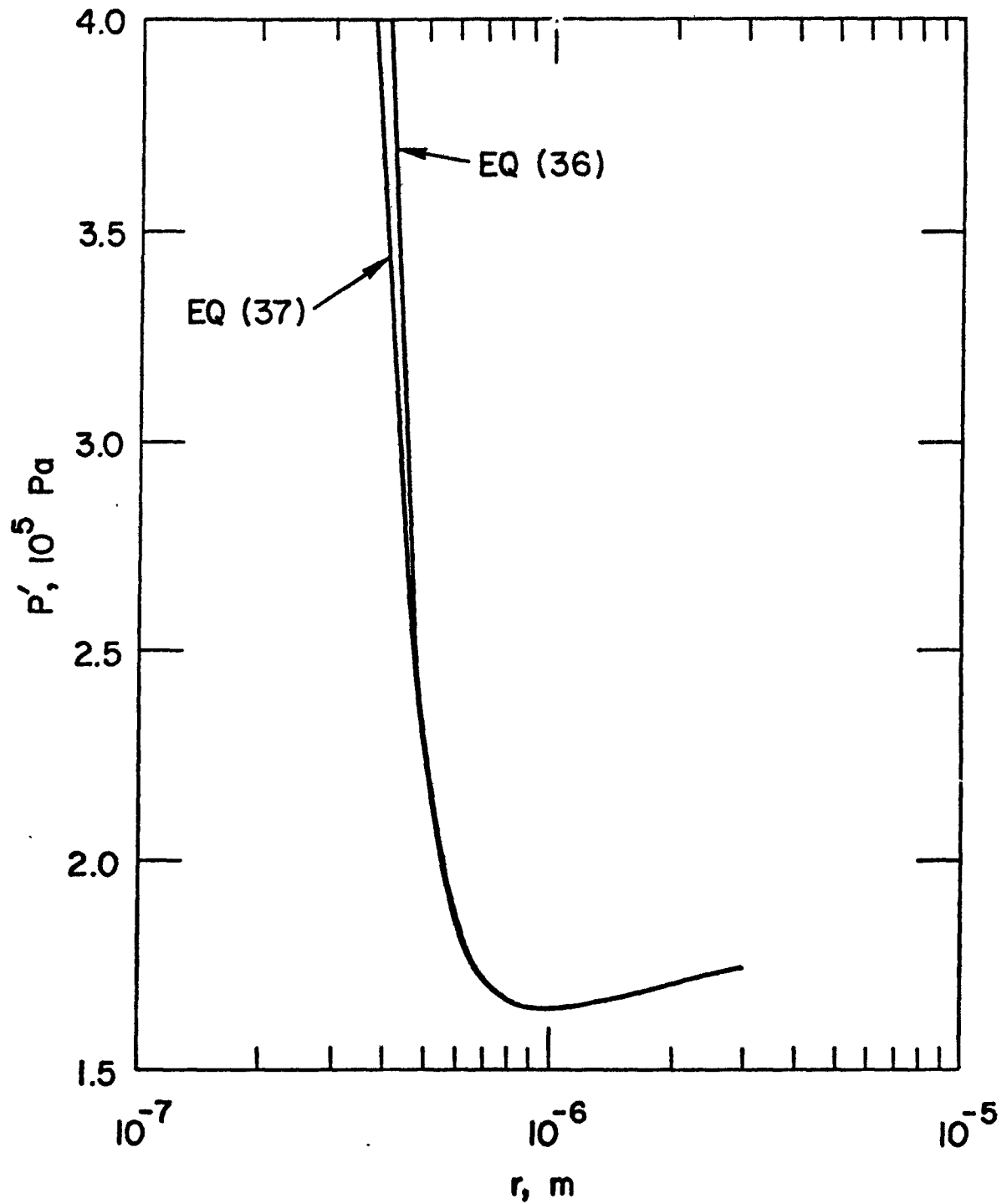


Fig. 8. Comparison between the stability boundary calculated by using equation (36) and the loci of maxima and minima calculated by using equation (37) for a CO_2 - Freon 21 system with $T = 298\text{K}$ and $N_1 = 10^{-14} \text{ g-mol}$.

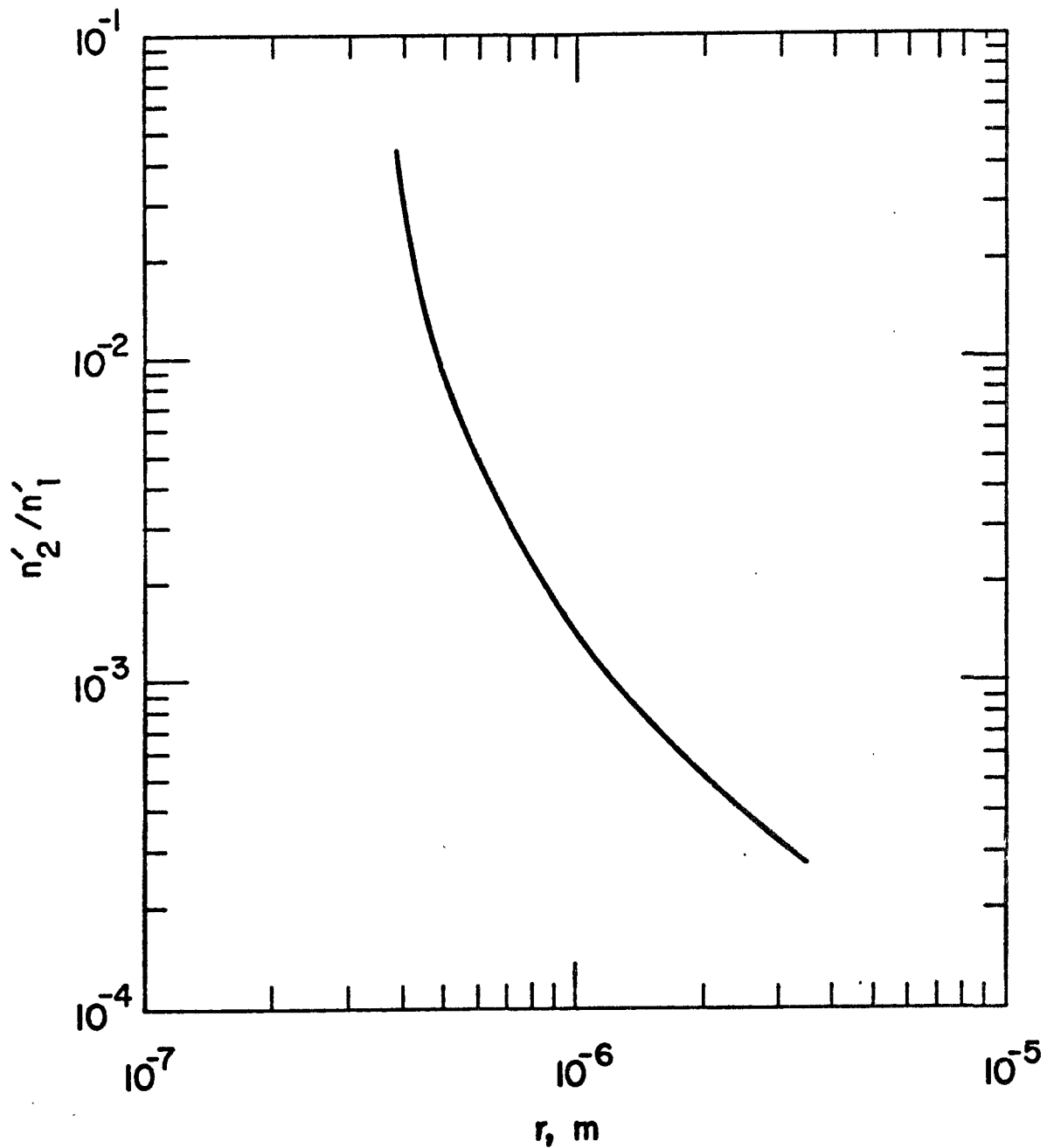


Fig. 9. Variation of n'_2/n'_1 with r for a CO_2 - Freon 21 system with $T = 298\text{K}$ and $N_1 = 10^{-14}$ g-mol.

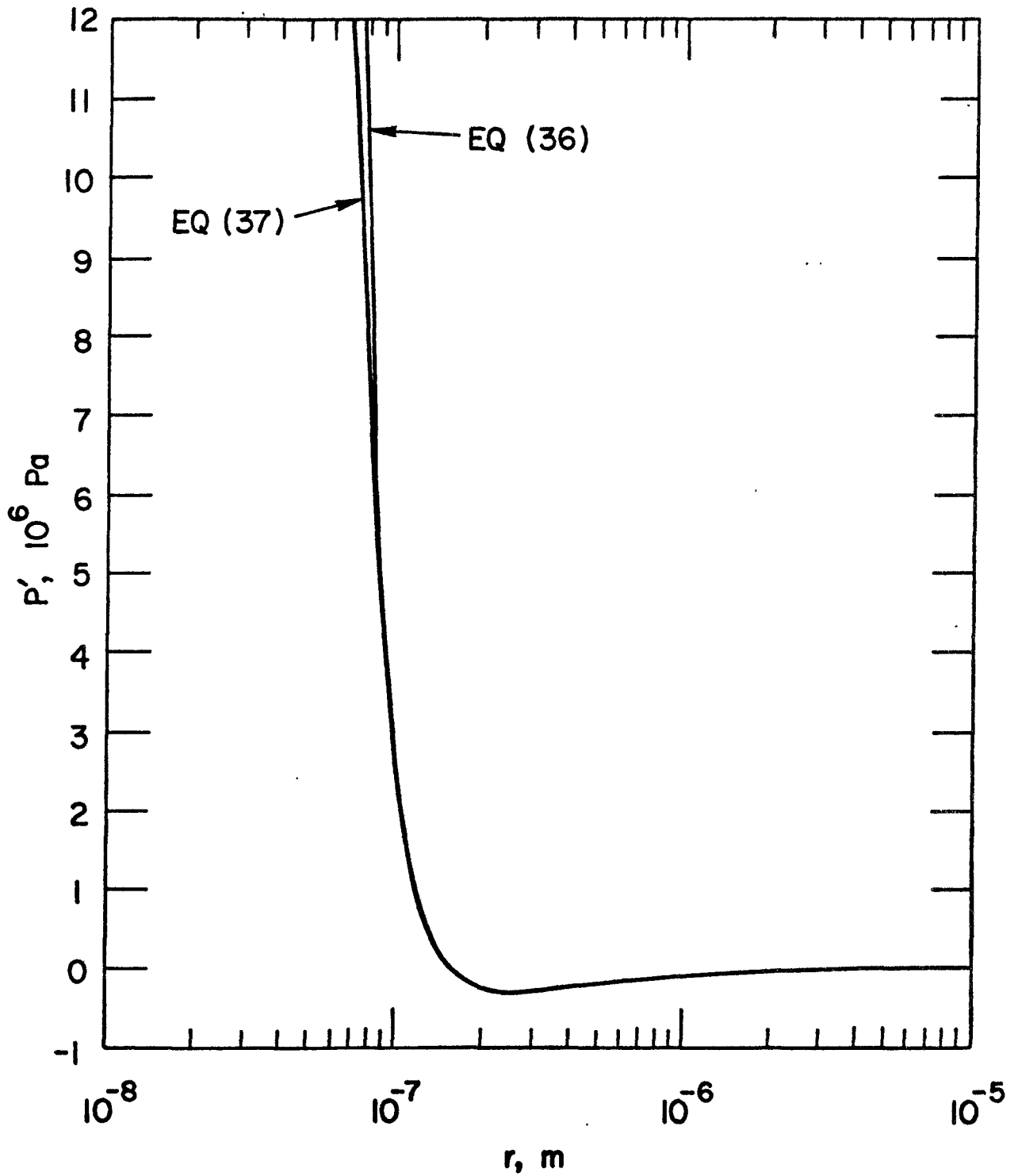


Fig. 10. Comparison between the stability boundary calculated by using equation (36) and the loci of maxima and minima calculated by using equation (37) for a $N_2 - H_2O$ system with $T = 293K$ and $N_1 = 10^{-14}$ g-mol.

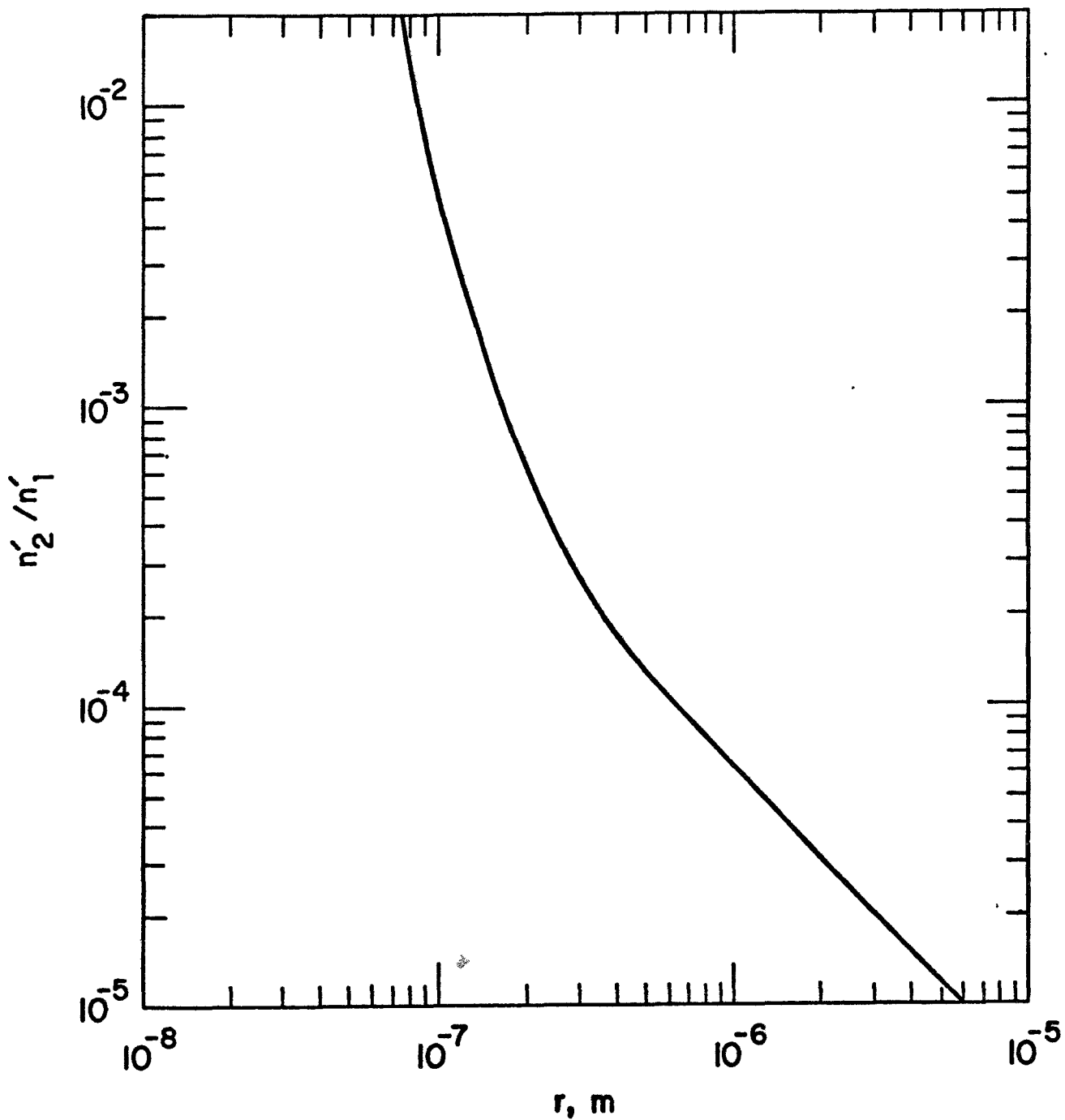


Fig. 11. Variation of n'_2/n'_1 with r for a $N_2 - H_2O$ system with $T = 293K$ and $N_1 = 10^{-14}$ g-mol.